European Geothermal Congress 2016
Strasbourg, France, 19-24 Sept 2016

New Bayesian formulation to integrate body-wave polarization in non-linear earthquake location

Emmanuel Gaucher[1], Alexandrine Gesret[2], Mark Noble[2] and Thomas Kohl[1]

[1] Karlsruhe Institute of Technology, Institute of Applied Geosciences, Geothermal Research, Karlsruhe, Germany

[2] MINES-ParisTech, PSL Research University, Geosciences Department, Paris, France

emmanuel.gaucher@kit.edu

Keywords: probability density function, location uncertainty, direction of arrival, induced seismicity, directional statistics.

ABSTRACT

Earthquake location is most of the time computed using arrival times of seismic waves observed on monitoring networks. However, three-component seismometers enable measurement of the seismic wave polarization which is also hypocentre dependent. Especially for local and sparse seismic networks, as can be encountered in local reservoir applications such as geothermal field monitoring, this information can be used in addition to the travel-times to better constrain the hypocentre of local earthquakes.

We propose a new Bayesian formulation for the likelihood function of an earthquake hypocentre associated with the P-wave polarization information. The formulation is consistent with directional statistics contrarily to existing ones. The whole information of the P-wave covariance matrix is used. The non-linearity of the location problem is kept with this approach. Hence, the polarization information can be treated at the same level as the time information to build a joint probability density function of the earthquake location. Earthquake hypocentres are therefore provided with a realistic uncertainty domain.

1. INTRODUCTION

Most of the time, earthquake location is still computed using the arrival times of the seismic waves observed on monitoring networks. However, given the increasing deployment of three-component seismometers, the direction of arrival of the seismic waves is often also available. Especially for local and sparse networks, as typically encountered in geothermal field monitoring, this information can be used in addition to the travel-time to better constrain the hypocentre of local earthquakes. As a matter of fact, the P-wave supporting ray may not reach the seismometer vertically thus providing hints on the hypocentre direction from the considered station.

The P-wave polarization has already been used to locate, however mainly when it was mandatory. A typical application is the monitoring of hydraulic fracturing for enhanced oil and gas recovery where the network often consists of a string of three-component seismometers deployed in a single well (Phillips *et al.* 1998; Oye and Roth 2003; Maxwell *et al.* 2010). The polarization of the P-wave is usually defined by its azimuth and inclination and most of the time the azimuth is used to locate. To our knowledge, only Kinscher *et al.* (2015) propose a non-linear and Bayesian formalism to define the probability density function of an earthquake hypocentre associated with both the azimuth and the inclination of the P-wave.

In the following, we first present the existing formulation and its limitations before describing the formulation we suggest to use. Then, synthetic tests in a 1D velocity model are performed to illustrate the new approach and to highlight its differences with the existing one.

2. THEORY

2.1. P-wave polarization

To quantify the polarization of the P-wave observed at a 3C-sensor, we use the standard approach of the covariance matrix of the signal (Flinn 1965; Montalbetti and Kanasewich 1970), which is computed for a time window around the wave arrival, after removal of the signal mean. If $\boldsymbol{x_i}$ is the signal amplitude vector measured on the three orthogonal components of the sensor at time i, then the covariance matrix $\boldsymbol{C}$ over p time samples is:

$$\boldsymbol{C} = \sum_{i=1}^{p} \boldsymbol{\bar{x}_i}^t \, \boldsymbol{\bar{x}_i} \quad [1]$$

where $\boldsymbol{\bar{x}_i}$ is the signal at time i corrected from its mean over the p time samples. The trace of the covariance matrix $\boldsymbol{C}$ corresponds to the mean energy of the signal in the considered time window. Principal component analysis of $\boldsymbol{C}$ allows identifying the three orthogonal principal directions of the signal polarization, corresponding to the eigenvectors $(\boldsymbol{v_1}, \boldsymbol{v_2}, \boldsymbol{v_3})$, as well as the associated amount of energy, corresponding to the eigenvalues $(\boldsymbol{\lambda_1}, \boldsymbol{\lambda_2}, \boldsymbol{\lambda_3})$. When all eigenvalues of the matrix $\boldsymbol{C}$ are equal, the signal is isotropic (i.e. not polarized); on the contrary, when one eigenvalue is much larger than the other two, the signal is linearly polarized along the corresponding eigenvector.

2.2. Existing probability density function

This direct P-wave is expected to be linearly polarized along the hypocentre-sensor seismic ray and thus brings relatively straight forward information about the earthquake incoming direction. Accordingly, to our knowledge, apart from Bardainne and Gaucher (2010), the existing methodologies based on the covariance matrix, take the direction of the eigenvector associated with the largest eigenvalue as the P-wave incoming direction (e.g. Phillips *et al.* 1998; Oye and Roth 2003; Kinscher *et al.* 2015). In practice, the main eigenvector is described by its azimuth θ and its inclination φ, in the geographical coordinate system. This approach is very common and in the Bayesian, non-linear, least-squares formulation proposed by Kinscher *et al.* (2015), the probability density function (PDF) of an earthquake hypocentre associated with a modelled polarization vector $\boldsymbol{P}(\theta_{cal}, \varphi_{cal})$ knowing the P-wave principal direction observed at one station $\boldsymbol{P}(\theta_{obs}, \varphi_{obs})$, is given by:

$$\mathcal{P}_{\mathcal{G}} = k \exp\left[-\frac{(\theta_{obs} - \theta_{cal})^2}{2\sigma_\theta^2} - \frac{(\varphi_{obs} - \varphi_{cal})^2}{2\sigma_\varphi^2}\right] \quad [2]$$

with σ_θ the uncertainty on the observed P-wave azimuth θ_{obs}, σ_φ the uncertainty on the observed P-wave inclination φ_{obs}, and k a normalizing constant.

Although equation [2] is attractive because it looks like the PDF associated with the time arrivals of the seismic waves (e.g. Tarantola and Valette 1982), it has several limitations which are also common to the linearized approaches. First of all, the polarization initially represented by the covariance matrix, is simplified by a single direction (i.e. the eigenvector associated with the largest eigenvalue), which is itself decomposed in two variables, azimuth and inclination that are taken independent although they should not. Second, quantifying the uncertainties of the azimuth and inclination of that vector appears difficult. Both uncertainties are often estimated from independent procedures that vary from author to author and are kept fixed at a given station for all earthquakes. Finally, the Gaussian form of equation [2] is not appropriate for angular data. As a matter of fact, the azimuth is a circular variable whose domain is in [0°, 360°] and the inclination is a variable whose domain is in [0°, 90°]. Both domains are not in the]-∞, +∞[as would be expected. Moreover, the meaning of angular uncertainties of ±∞ (for σ_θ and σ_φ) as suggested by equation [2] is difficult to explain physically.

To prevent such issues, we propose a new Bayesian formulation which keeps the whole information contained in the covariance matrix and which keeps the polarization as a directional data.

2.3. Proposed probability density function

The use of the covariance matrix $\boldsymbol{C}$ to quantify the polarization of the P-wave implies that the spatial distribution of the seismic amplitudes around this wave arrival follows a trivariate Gaussian distribution centred on 0: $\boldsymbol{x} = \mathcal{G}(\boldsymbol{0}, \boldsymbol{C})$ (as emphasized by the principal component analysis which can be made on $\boldsymbol{C}$). Following the work of Tyler (1987) on spherical data and according to Mardia and Jupp (2000), this property allows describing the distribution associated with the variable $\boldsymbol{u} = \boldsymbol{x}/\|\boldsymbol{x}\|$ by:

$$\mathcal{P}_{\mathcal{ACG}} = \frac{\Gamma\left(\frac{3}{2}\right)}{\sqrt{(2\pi)^3|\boldsymbol{C}|}} \left(\boldsymbol{u}\,\boldsymbol{C}^{-1}\,\boldsymbol{u}^t\right)^{-\frac{3}{2}} \quad [3]$$

where $\boldsymbol{u}$ represents the 3D signal divided by its amplitude, Γ the gamma function. $\boldsymbol{u}$ can be seen as the instantaneous direction of arrival of the signal. This $\mathcal{P}_{\mathcal{ACG}}$ distribution is called the angular central Gaussian (ACG) distribution and it gives the likelihood that any unitary vector $\boldsymbol{u}$ is well represented by the distribution defined by the statistical sample $\boldsymbol{x}$. Therefore, it can also define the probability density function of an earthquake hypocentre associated with the polarization observed at a given station in a given time window and represented by the covariance matrix $\boldsymbol{C}$, and a modelled direction of arrival of the P-wave $\boldsymbol{u}$.

The ACG distribution is consistent with Gaussian distribution of the original seismic signal and perfectly suits the objective of working with unitary vector variables representing the direction of arrival of the P-wave instead of scalar variables. It has the property to be adapted to axial distributions, by opposition to directional distributions: $\mathcal{P}_{\mathcal{ACG}}(\boldsymbol{u}) = \mathcal{P}_{\mathcal{ACG}}(-\boldsymbol{u})$. This is justified because the polarity of the P-wave arrival cannot be determined at a station prior to the earthquake location. Moreover, $\mathcal{P}_{\mathcal{ACG}}(\boldsymbol{C}) = \mathcal{P}_{\mathcal{ACG}}(q\boldsymbol{C})$, for any positive scalar q, which means that the mean energy of the P-wave is not taken into account, only its spatial distribution. As a consequence, low or high magnitude earthquakes are processed the same way. The constant values in equation [3] assure that the integral of the probability density over the sphere (i.e. all possible directions) is one, in other words, that the probability density function is well normalized. The ACG formulation uses the whole covariance matrix without any pre-processing step like principal component analysis and therefore keeps the spatial dependencies of the P-wave signal and includes uncertainties of observation.

3. SYNTHETIC FIELD CASE

To illustrate the capabilities of the proposed ACG formulation and to show the differences with the least-squares formulation, as proposed by Kinscher *et al.* (2015), we generate a synthetic field case.

In this numerical example, the seismic network consists of a string of five 3C-sensors deployed in one vertical well between 100 m and 300 m. The interspacing distance between the sensors is 50 m (Figure 1). The velocity model is represented by three flat layers with homogeneous P-wave velocities in the range of 3800 m/s to 5000 m/s. The second layer has the lowest velocity and contains the middle sensor of the seismic string. A synthetic earthquake source is positioned 100 m below the seismic string at an offset of 300 m. Such a synthetic field case may be representative of downhole geothermal field monitoring or hydraulic fracturing monitoring.

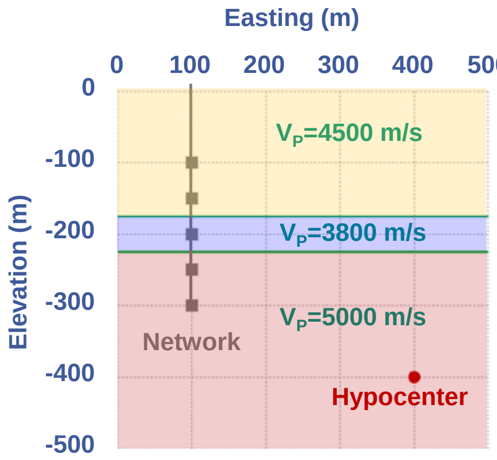

Figure 1: Geometry of the synthetic field case.

To compute the theoretical direction of P-wave arrival from any point in the location zone to each 3C-sensor, the accurate 3D finite-difference code of Noble, Gesret and Belayouni (2014) is used. Hence, the vector $\boldsymbol{u}$ of equation [3] or its azimuth θ_{cal} and inclination φ_{cal} in equation [2] is available. To simulate the observed P-wave direction at the 3C-sensors in equation [2] (i.e. θ_{obs} and φ_{obs}), we take the theoretical angles associated with the exact hypocentre location and fix the angles uncertainties (i.e. σ_θ and σ_φ). For equation [3], a covariance matrix $\boldsymbol{C}$ is generated with a principal direction $\boldsymbol{v_1}$ equals to the theoretical source-station direction and with eigenvalues such that $\lambda_1 = 1$, $\lambda_2 = \sin^2(\sigma_\theta)$ and $\lambda_3 = \sin^2(\sigma_\varphi)$. Accordingly, if $\sigma_\theta = \sigma_\varphi = 90°$, $\boldsymbol{C}$ correspond to an isotropic incoming wave and if $\sigma_\theta = \sigma_\varphi = 0°$, $\boldsymbol{C}$ is a perfectly linear signal.

With such a field design and the associated synthetic data, $\mathcal{P}_{\mathcal{G}}$ and $\mathcal{P}_{\mathcal{ACG}}$ are estimated everywhere in the location zone.

3.1. Single station location

To start with, only the upper station is used to locate the synthetic source. Figure 2 displays the location probabilities by displaying three contours delimiting the 68.3%, 95.4% and 99.7% location probability volumes. Both formulations points toward the correct hypocentre location, however, discrepancies increase with increasing location probability: although the 68.3% contour looks relatively similar in both cases, major differences appear for the 95.5% and the 99.7% domains. The 99.7% probability volume for the earthquake location covers almost the whole space with the ACG formulation, which is expected for a single station location. On the contrary, the least-squares formulation covers a much smaller volume at 99.7% probability, independently of the inclination uncertainty value ($\sigma_\varphi = \pm 90°$ or $\sigma_\varphi = \pm 10°$). Hence, the least-square formulation is too optimistic and provides unexpected small location uncertainty domains. This results from the inherent inconsistency of the least-squares formulation which should set $\sigma_\varphi = \pm\infty$ in equation [2] for total lack of knowledge of the angle but which would not be physically related to the angle domain [0°, 360°] any longer. This issue does not exist in the ACG formulation. In case of undetermined inclination ($\sigma_\varphi = \pm 90°$), all contours obtained by the least-squares formulation are almost vertical. This emphasizes the effect of considering as independent the azimuth and inclination angles.

3.2. Seismic string location

The five 3C-sensors of the seismic string are now used to locate the synthetic event. Figure 3 shows the results for the pair of angle uncertainties $\sigma_\theta = \pm 10°$, $\sigma_\varphi = \pm 10°$. As observed, the ACG formulation constrains the earthquake location around its expected position better than the least-square formulation. This is because the ACG formulation keeps the intrinsic correlation between the azimuth and the inclination of the P-wave direction of arrival (in the covariance matrix), which brings more information to solve the inverse problem.

We simulated with this synthetic example a perfect-data case to highlight the intrinsic properties of the ACG formulation and to fairly compare the latter with an existing formulation. Of course, any issue and pitfall of using the covariance matrix measured on 3C-sensors to locate earthquakes is not removed by using the ACG formulation (or any other formulation).

4. CONCLUSIONS

We propose to use the angular central Gaussian formulation to integrate P-wave polarizations in non-linear earthquake location. We compared this Bayesian formulation to the existing but physically incorrect least-squares formulation. The ACG formulation treats the direction of arrival of the P-wave as a unitary vector and places it in a spherical system as it should. It uses the full covariance matrix of the P-wave which does not need to be further processed and simplified to one single principal vector as usually done. The simple formulation offers an "all-in-one" solution including spatial dependencies and uncertainties. The probability density function of the earthquake hypocentre defined through the ACG formulation is consistent with Gaussian statistics, well normalized and gives correct estimate of a posteriori uncertainty. This allows its direct combination with other probability density functions such as those associated with the arrival times.

The proposed non-linear approach is particularly adapted to local and sparse seismological networks which necessitate the use of information such as P-wave polarization to better constrain the earthquake locations. Hence, it could typically be applied in geothermal fields or in enhanced oil and gas recovery, and it could be used to orient 3C-sensors from an known seismic source.

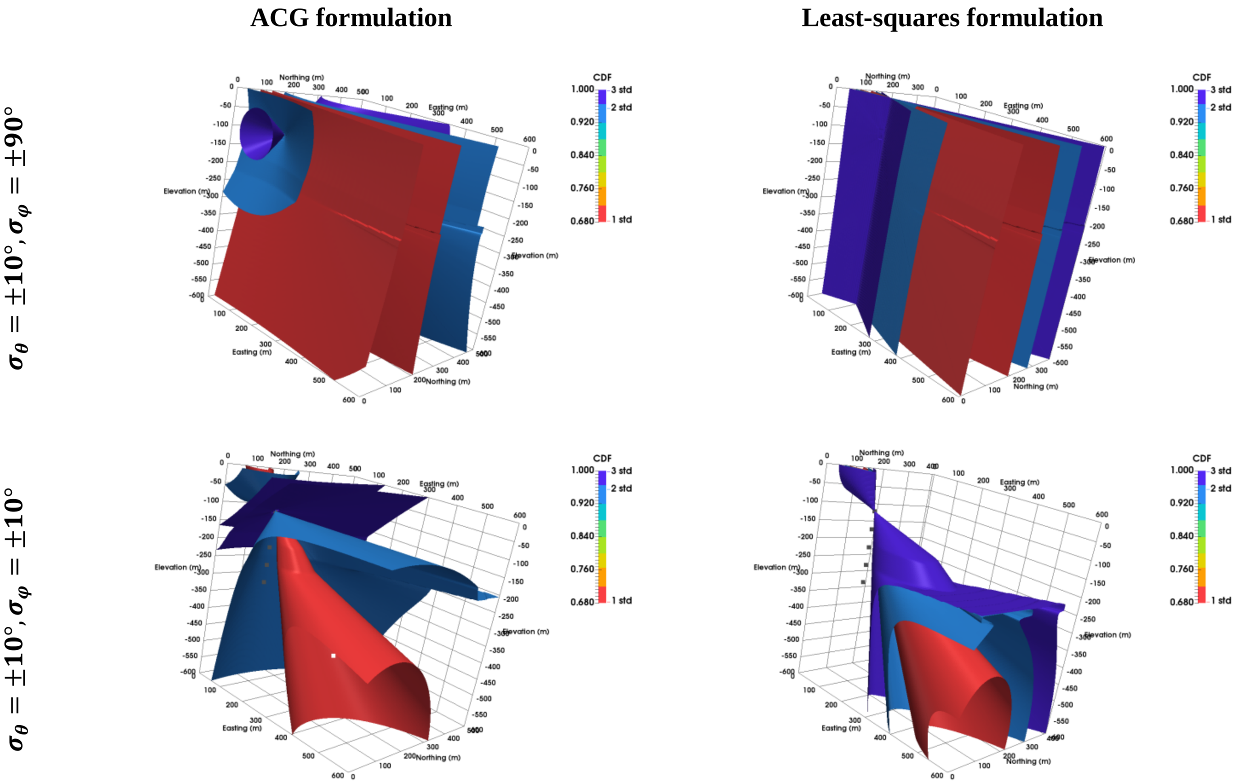

Figure 2: Location probability of the synthetic source hypocentre (white square) computed from the upper 3C-sensor only (grey cube). The contours delimiting the 68.3% (red), 95.5% (light blue) and 99.7% (dark blue) probabilities are displayed. The left and right columns show the results from the ACG and the least-squares formulations respectively. The upper and lower rows show the results for the pairs of angular uncertainties ($\sigma_\theta = \pm 10°, \sigma_\varphi = \pm 90°$) and $\sigma_\theta = \pm 10°, \sigma_\varphi = \pm 10°$) respectively.

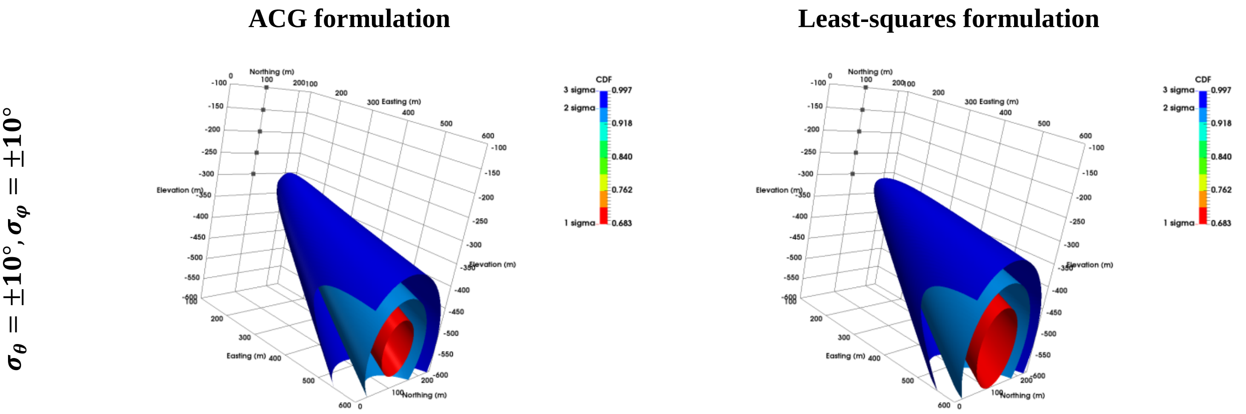

Figure 3: Location probability of the synthetic source hypocentre computed from the five 3C-sensor of the seismic string. Same representation as Figure 2.

REFERENCES

Bardainne T. and Gaucher E. 2010. Constrained tomography of realistic velocity models in microseismic monitoring using calibration shots. *Geophysical Prospecting* **58** (5), 739–753.

Flinn E.A. 1965. Signal analysis using rectilinearity and direction of particle motion. *Proceedings of the IEEE* **53** (12), 1874–1876.

Kinscher J., Bernard P., Contrucci I., Mangeney A., Piguet J.P. and Bigarre P. 2015. Location of microseismic swarms induced by salt solution mining. *Geophysical Journal International* **200** (1), 337–362.

Mardia K.V. and Jupp P.E. 2000. *Directional statistics.* Wiley. ISBN 0471953334.

Maxwell S.C., Rutledge J., Jones R. and Fehler M. 2010. Petroleum reservoir characterization using downhole microseismic monitoring. *Geophysics* **75** (5), 75A129-75A137.

Montalbetti J.F. and Kanasewich E.R. 1970. Enhancement of Teleseismic Body Phases with a Polarization Filter. *Geophysical Journal of the Royal Astronomical Society* **21** (2), 119–129.

Noble M., Gesret A. and Belayouni N. 2014. Accurate 3-D finite difference computation of traveltimes in strongly heterogeneous media. *Geophysical Journal International* **199** (3), 1572–1585.

Oye V. and Roth M. 2003. Automated seismic event location for hydrocarbon reservoirs. *Computers & Geosciences* **29** (7), 851–863.

Phillips W., Fairbanks T., Rutledge J. and Anderson D. 1998. Induced microearthquake patterns and oil-producing fracture systems in the Austin chalk. *Tectonophysics* **289** (1–3), 153–169.

Tarantola A. and Valette B. 1982. Inverse problems = quest for information. *Journal of Geophysics* **50**, 159–170.

Tyler D.E. 1987. Statistical analysis for the angular central Gaussian distribution on the sphere. *Biometrika* **74** (3), 579–589.

Acknowledgements

Most of this work was conducted in the frame of the German LFZG joint project “Kombiniertre Voruntersuchungen für Tiefengeothermie-Labor” (#L75 14001) which was supported by the PTKA, the BWPLUS program and the Ministry of the Environment, Climate Protection and the Energy Sector – Baden-Württemberg. This work was also partly funded by the EnBW Energie Baden-Württemberg AG.